Annals of Nuclear Energy 83 (2015) 50–56

Contents lists available at ScienceDirect

Annals of Nuclear Energy

journal homepage: www.elsevier.com/locate/anucene

Investigation of the pulse energy noise dynamics of IBR-2M using cluster analysis

Yu.N. Pepelyshev [a,*], Ts. Tsogtsaikhan [a,b]

[a] Joint Institute for Nuclear Research, 141980 Dubna, Moscow region, Russia
[b] Institute of Physics and Technology, MAS, Mongolia

ARTICLE INFO

Article history:
Received 4 August 2014
Received in revised form 16 March 2015
Accepted 2 April 2015
Available online 24 April 2015

Keywords:
IBR-2M
Pulse energy
Cluster analysis
Power spectrum

ABSTRACT

In this work we present the results of a study on pulse energy noise dynamics of the IBR-2M; the study employs statistical methods of time series (pulse energy) processing and hierarchical cluster analysis. It is shown that the power spectrum changes of the pulse energy fluctuations per cycle (~11 days) has a transition region duration of ~3 days that takes place after the reactor has reached the nominal power of 2 MW. The power noise is subsequently divided into four stable clusters, with three of which describe the noise transition region. The fourth cluster constitutes a stable structure that does not depend on noise level (amplitude of the power spectrum) or on reactor operation time. The noise transition region is formed by the vibration of the moving reflectors once the reactor has been reached.

1. Introduction

The key feature of the IBR-2M reactor, as compared to the steady-state reactor, is its high sensitivity to external reactivity perturbations; these perturbations can be up to 40 times higher than those of steady-state reactors using uranium fuel. The pulse energy noise of the IBR-2M reactor – which is caused by the operation of various technological systems, including the reactor core cooling system and the moving reflectors, directly affects the safety as well as the reliability of reactor operation. Owing to the high sensitivity of the reactor to reactivity perturbations, the total pulse energy noise may reach ±22% in the stabilization mode. The pulse energy noise constitutes one of destabilizing factors of the IBR-2M reactor in that the degradation processes which occur in the core and its vicinity during the operation of the reactor cause a change in the level as well as the structure of the noise. During this mode, the investigation and analysis of the reactor noise variation dynamics is most important for ensuring the safety as well as the reliable operation of the reactor. To this end, the dynamics of the pulse energy noise at the IBR-2M has been investigated using cluster analysis. The hierarchical cluster algorithm is used here as it is more flexible than other methods, thus allowing (a) a detailed study of the structure and differences in pulse energy values, and (b) the selection of the optimal number of clusters. In this piece of research, the results of this analysis are presented, based on statistical methods of time series processing and hierarchical cluster analysis.

During the 1980's and 90's, pattern recognition methodologies and, in particular, cluster analysis were used widely for the study of the IBR-2 and its condition diagnostics (Gonzalez et al., 1974; Pepelyshev and Dzwinel, 1990a,b, 1991, 1992, 1994; Pepelyshev et al., 1994). These methods permitted the investigation of very fine and weak reactivity perturbations that could not be observed and investigated with any other method. With advent of powerful computation systems and cluster analysis methods, the application of the aforementioned methods to the upgraded IBR-2M reactor is again of major importance.

2. Goal of the work and data processing procedure

The goal of this work is to investigate the dynamics of the pulse energy noise at the IBR-2M during a reactor cycle. The reactor cycle can be described as: operation for two weeks at a power of 2 MW; power drop to almost zero, and an interruption in operation for a week; periodical repetition of this cycle, with the regime chosen in such a manner as to meet the needs of the experiment (neutron beams).

2.1. Brief description of the IBR-2M reactor

The IBR-2M reactor is located in Dubna (Moscow region, Russia), and operates with a design power of 2 MW. The IBR-2M core capacity is 69 fuel elements, which are sleeve-like PuO_2

* Corresponding author at. Institute of Physics and Technology, MAS, Mongolia. Fax: +7 (09621) 6 51 19.
E-mail address: pepel@nf.jinr.ru (Y.N. Pepelyshev).

http://dx.doi.org/10.1016/j.anucene.2015.04.012
0306-4549/

pellets. The coolant is liquid sodium, pumped through the emergency protection blocks by two induction pumps. There are two aligned blades rotating with different speeds past one of the core faces. They are the main movable reflector (MMR) and the auxiliary movable reflector (AMR) of the reactivity modulator. The MMR rotor is a three-tooth blade with a counterbalance, and the AMR rotor is a two-tooth blade. The reactivity level is adjusted by the control and protection system (CPS) elements, which are movable tungsten blocks in an array of fixed steel reflectors. The arrangement of the CPS elements with respect to the IBR-2M core is shown in Fig. 1.

The IBR-2M is a periodic-pulse fast reactor, with periodically repeated power pulses. The key feature of the IBR-2 reactor is the presence of a mechanical reactivity moderator – a moving reflector that allows for a cyclic process of deep change of reactivity. The IBR-2 reactor can be transferred with period of 0.2 s from a deeply subcritical ($k_{ef} \approx 0{,}97$) state into a supercritical state on prompt neutrons in less than 1 ms. As a result, the reactor generates powerful neutron pulses with a period of 200 ms. In the intervals between pulses (i.e., when there are neither MMR nor AMR in front of the core), the reactor (background) power is approximately four orders of magnitude lower than the power pulse amplitude. Owing to that principle of the pulsing reactivity formation, almost the total release of energy in the reactor takes place during power pulses (93%), with the fraction of pauses being as low as 7% of the total energy.

Since, as already mentioned, the IBR-2M sensitivity to reactivity perturbations is high, the pulse energy has a considerable spread. Sources of random reactivity perturbations include the moving reflectors, vibrations of fuel elements in the turbulent flow of sodium, as well as vibrations induced by the operation of various technological systems. Reactivity noise is one of the destabilizing factors when controlling a reactor. From a safety point of view, the reactivity noise can be divided into two large groups: (a)-high-frequency noise (over ~ 0.03 Hz) that is due to the power feedback and power stabilization system; and (b) low-frequency noise (below the defined frequency). While the reactivity perturbations from (a) cause pulse energy fluctuations, those from (b) lead to fluctuations in the automatic regulator, which is a high fluctuation in reactivity that can go beyond the stabilization zone.

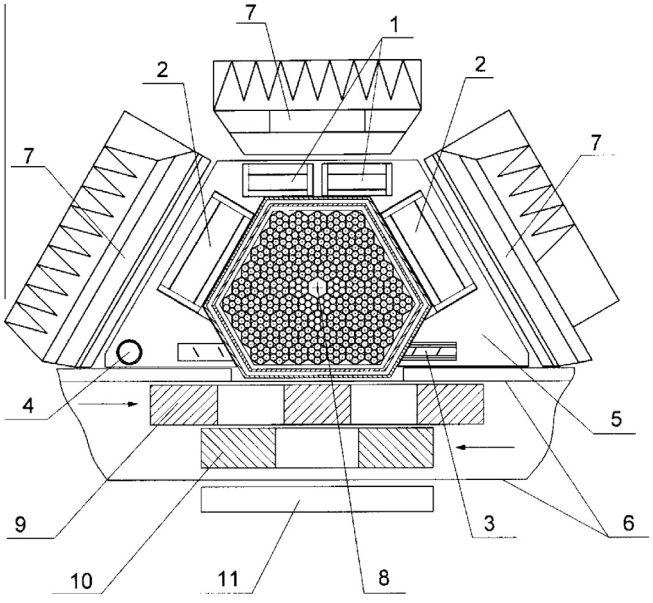

Fig. 1. Cross-sectional view of the IBR-2M core: (1) emergency protection blocks, (2) compensation block, (3) intermediate control block, (4) automatic regulator, (5) stationary reflector, (6) movable reflector case, (7) grooved water moderators, (8) external neutron source, (9) main movable reflector (MMR), (10) auxiliary movable reflector (AMR), (11) flat water moderator.

Pulse energy amplitudes were investigated via repeated measurements of three independent detectors arranged around the core. The current integral corresponding to the power pulse was measured for one of these detectors, showing a detector signal proportional to the pulse energy. Note that, in the power mode of operation (i.e., at the equilibrium pulse criticality), the pulse amplitude and energy are equivalent; the relationship between them can change only if the rotation phase of the main and auxiliary movable reflectors changes for some reason. Hence, the current pulse integral was measured for verifying the main measurements. Each successive power pulse was measured in one of the typical reactor cycles in 2013 with the sodium flow through the core 100 m^3/h. The measurements were carried out for 10.5 days, beginning with the moment when the reactor reached the power of 2 MW and ending with the power drop at the conclusion of the cycle. The recorded time series, that included $\sim 10^7$ successive pulse energy values, was processed using statistical and cluster analysis procedures. The main element of the statistical analysis was the spread of values, and the object of the cluster analysis was the power spectrum of pulse energy fluctuations. The basic analysis procedures for the measured data are presented below.

2.2. Power spectrum of pulse energy fluctuations and pulse energy spread

The total time series (pulse energy) $X(t)$ recorded within the entire reactor cycle was divided into successive time series X_i with a length of 8192 (or ~28 min). For each time series X_i a finite Discrete Fourier transform was calculated via the periodogram method. The power spectrum of the reactor pulse energy fluctuations $S_X^{(i)}(f)$ was determined as

$$|S_X^{(i)}(f)|^2 = F[X_i(t)]^2$$

where F is the Fourier transform operator. The following parameters of the spread of elements entering into the time series X_i were investigated: $\sigma_{f_j}^2$, dispersion of fluctuations at the average frequency f_j; σ_f^2, total dispersion calculated from the spectrum; $\sigma_t/\bar{Q}$, relative standard variation ($\bar{Q}$ is the average pulse energy); σ_t, standard pulse energy deviation calculated in the time domain; and the relative partial root-mean-square deviation

$$\eta_j = \left(\sqrt{\frac{\sigma_{f_j}^2}{\sigma_f^2}} \right) \cdot \frac{\sigma_t}{\bar{Q}} \cdot 100\%$$

2.3. Cluster analysis

In the present case, the objective of the cluster analysis was to classify a great amount of IBR-2M noise state data. Various cluster analysis methods (both hierarchical and non-hierarchical) were used. Hierarchical cluster analysis, which is the most flexible of the existing cluster analysis methods, allows the structure of the dissimilarities between objects (between the points) to be investigated, and the optimum number of clusters to be chosen. The non-hierarchical algorithms have been used in addition to the hierarchical ones due to their built-in heuristic data analysis procedures, as for example – in the ISODATA algorithm (Gonzalez et al., 1974), which produced a more significant (large) number of clusters. Each successive power spectrum of the pulse energy fluctuations (hereinafter referred to as the spectrum) reflecting the reactor noise state in the time interval of ~28 min (or 8192

successive pulse energy values) was represented by a point in the multidimensional Euclidean space. The Euclidean distance between the ith and kth points is given by

$$d_{ik} = \left[\sum_{j=1}^{p}(x_{ij} - x_{ik})^2\right]^{\frac{1}{2}}.$$

The aforementioned power spectrum of the IBR-2M pulse energy fluctuations was used in one of the typical reactor cycles in 2013. The dimension of the space was 256 coordinates, i.e. the number of points in the spectrum. The chosen cluster analysis methods are based on the analysis of the distances between the points. The measure of similarity is the minimum distance between the points in the cluster. The square of the Euclidean distance and the absolute value of the distance between the points were also investigated as an alternative distance. The greatest difficulty in the investigation of the dynamic variation in the object structure using the cluster analysis is to determine the "correct" number of clusters. All clustering algorithms are based on the assumption that the initial distribution of objects (in our case, spectra) is not uniform in the space with the chosen measure of length (Boldak and Sukharev, 2011); In other words, clustering is possible only if the initial data allow it. There are a few heuristic clustering algorithms capable of automatically determining the number of clusters. (Goujun et al., 2007), but this is not adequate in this case, since these algorithms are based on formalized analysis procedures and therefore require either that additional a priori data be introduced or that acceptable criteria for evaluation of results are used. As stated in Boldak and Sukharev (2011), there are at least 16 known criteria for evaluating the "correct" number of clusters. In the analysis of the IBR-2M noise structure all of these criteria, with a few exceptions, yield similar results. Adjusted Rand, Krzanowski-Lai, Hartigan, R-Squared indexes (Wang et al., 2009) may not effectively find the correct number of clusters in a data set when used independently. We used three criteria to evaluate the quality of the cluster structure. These three criteria have a high accuracy and does not directly depend on the number of clusters. Silhouette values offer the advantage that they depend only on the partition of the elements. As a consequence, silhouettes can be used to compare the output of the same clustering algorithm applied to the same data but for different numbers of clusters. For these criteria greater value indicates a higher quality of cluster structure. The first clustering "correctness" criterion was Dunn index $MD(c) = min(r(j,i))/max(Dk) \forall i,j,k: \ i \neq j$, where Dk is the cluster diameter, $r(j,i)$ is the distance between clusters i and j, and c is the number of clusters. The Dunn index allows compactness and separability of clusters to be evaluated (Dunn, 1974). The second obligatory condition for the analysis was an evaluation of the "silhouette", which is calculated for the ith point as $sw_i = \frac{(b_i - a_i)}{max(a_i, b_i)}$, where a_i is the average distance from all other points in its (the ith point's) cluster, $d(i,c)$ is the average distance relative to all points in cluster c, and $b_i = min\ d(i,c)$ (Rousseeuw, 1987). If the silhouette value averaged over all points is $\overline{sw} = \frac{1}{n}\sum_{i=1}^{n} sw_i > 0.5$, then the partition of the objects into clusters is meaningful; conversely, if $\overline{sw} < 0.2$, then the data do not have a cluster structure. Thus, choosing the number of clusters using the Dunn index and the silhouette is a necessary but not sufficient criterion. Fig. 2 shows how the average silhouette varies with the number of clusters in some of the cluster analysis methods.

The third criterion for evaluating the optimum number of clusters used in our work is based on the physical meaning of the clustering results. Physically, and provided that it is possible to partition spectra into clusters, these clusters should have an invariant attribute, i.e. a stable attribute with respect to the total reactor noise variation. Hence, the optimum algorithm for clustering spectra of IBR-2M pulse energy fluctuations is actually such

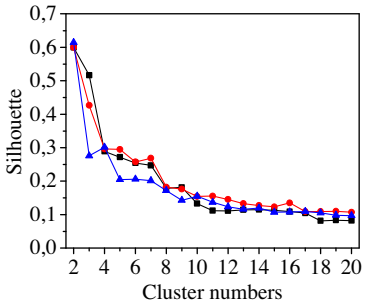

Fig. 2. Variation in the silhouette with the number of clusters in some of the cluster analysis methods: (■) weighted pair-group average, (▲) k-means, (●) unweighted center of mass distance (complete).

that the time sequence of the spectra has only a few "shifts" to the neighboring clusters at relatively high values of the Dunn index and the silhouette. When choosing the optimum structure of the cluster, the following clustering procedures were used: the furthest neighbor method, weighted pair-group average, weighted center of mass distance, least squares method (Ward's method), and shortest distance (single), weighted center of mass distance (Goujun et al., 2007; Lawrence Hubert et al., 2009). The best results were obtained using the algorithm with solution of the minimax problem based on the weighted pair-group average and the Euclidean distance (Goujun et al., 2007). Finally, the clusters with minimum distances between the points in the cluster at the average distances between the cluster centers was selected. Fig. 3 shows the scheme of the hierarchical clustering algorithm used for the calculation. The weighed group average method is also referred to as the "Weighted Pair-Group Method Using Arithmetic Averages". Using the Lance–Williams formula, the distance between clusters is given by Goujun et al. (2007)

$$D(P \cup E, C) = \frac{D_{P,C} + D_{E,C}}{2}$$

where $P \cup E$ merged clusters, $D_{P,C}$, $D_{E,C}$ distance between $P \cup E$ and C clusters.

3. Main experimental results – analysis

Fig. 4 shows the variation in the power spectrum of IBR-2M pulse energy fluctuations per working cycle from the point in time where the power of 2 MW was reached to the point in time when power began decreasing. The power spectrum of pulse energy fluctuations, averaged over the entire cycle, is presented in Fig. 5. As is evident from Figs. 4 and 5, several high-intensity peaks are evident in the power spectrum.

The largest variations occur at the frequencies of 0.82 and 1.4 Hz. The peaks in the frequency ranges 0.78–0.85 and 1.36–1.80 Hz, as is shown above, are due to the axial (normal to core surface) vibrations of the MMR and AMR blades (Pepelyshev, 1987; Anan'ev et al., 2012a,b). The dominant pulse energy fluctuations at the frequencies of the axial vibrations of the movable reflectors are shown in Fig. 5, and account for ~55% of the total noise dispersion (Anan'ev et al., 2012a,b). The other harmonic oscillation components in the IBR-2 noise spectra are weak and close to the random background level. As becomes evident from Fig. 4, the power spectrum of the pulse energy fluctuations changes substantially during reactor operation. Fig. 6 shows the variation in the root-mean-square total pulse energy fluctuations as well as the fluctuations that are due to the vibrations of the MMR and AMR blades in the frequency ranges given in Fig. 5.

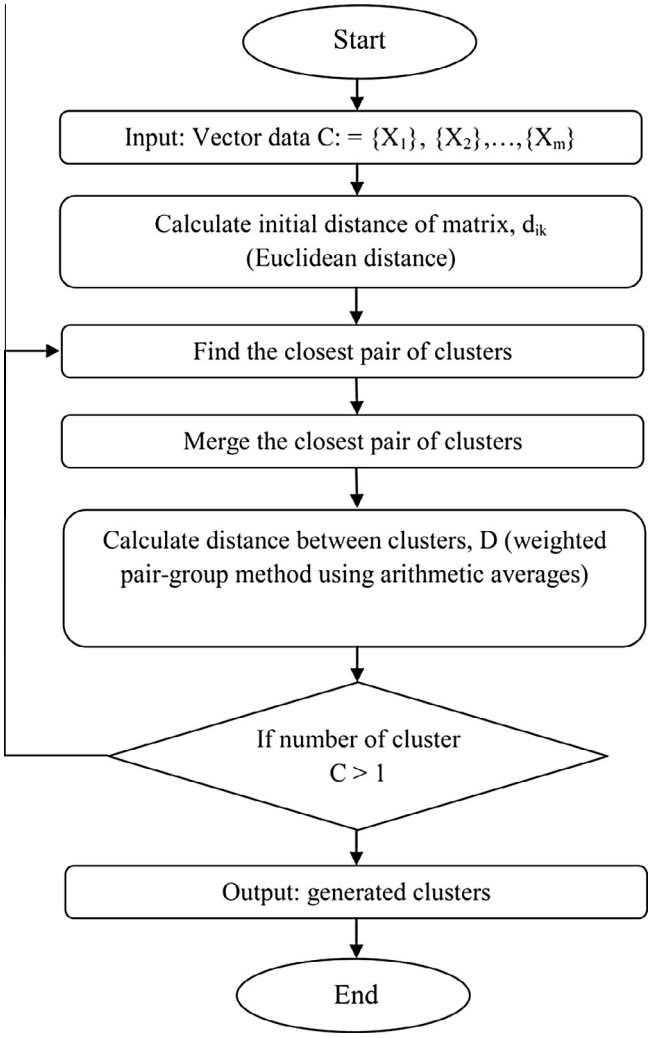

Fig. 3. The scheme of the hierarchical clustering algorithm.

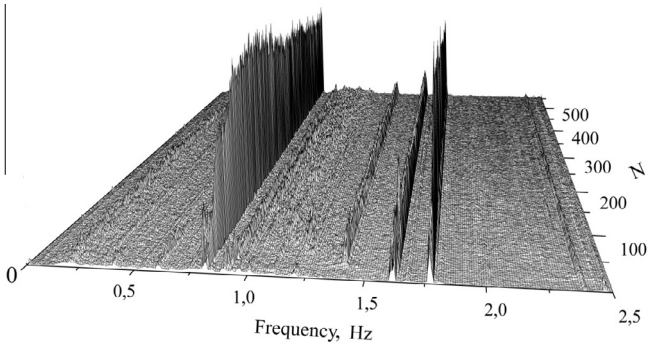

Fig. 4. Variation in the power spectrum of the IBR-2M pulse energy fluctuations per working cycle from the time of reaching the power of 2 MW to the time when power begins decreasing. The measurement duration is 10.5 days; 552 spectra are presented.

Fig. 6 also shows the sequence of cluster exchange in time for total pulse energy fluctuations and for fluctuations due to vibrations of the MMR and AMR blades. It becomes evident from Fig. 6 that the power spectrum of the pulse energy fluctuations is divided into four clusters. The first three clusters include spectra of the transition region that lasts 1.7 days after the reactor reaches

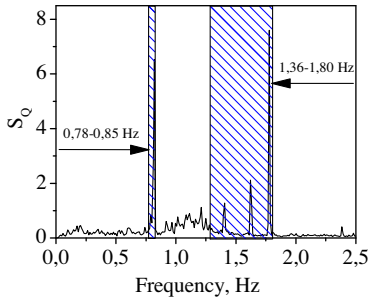

Fig. 5. Cycle-average power spectrum of IBR-2M pulse energy fluctuations (S_Q) at a power of 2 MW and sodium flow of 100 m^3/h. The dashed areas are associated with the vibrations of the movable reflectors.

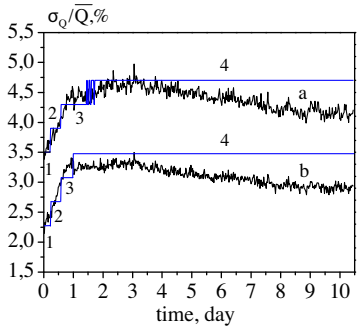

Fig. 6. Variation in the relative root-mean-square deviation of the total pulse energy fluctuations (a), and of those due to the axial vibrations of the MMR and AMR blades (b). The line shows the transition of the reactor noise state from one cluster to another. The numbers illustrate to the cluster numbers.

Table 1
Characteristics of the reactor noise state clusters in the process of the reactor operation.

Cluster No.	Analysis by total pulse energy fluctuations		Analysis by pulse energy fluctuations due to axial vibrations of MMR and AMR blades	
	Number of spectra in cluster	Cluster lifetime after 2-MW power is reached	Number of spectra in cluster	Cluster lifetime after 2-MW power is reached
1	13	0–5 h	12	0–6 h
2	18	5–14 h	19	6–14 h
3	22	14–41 h (1.2 d)	52	14–24 h (1 d)
4	499	1.7–10.5 d	469	1–10.5 d
Total	552	10.5 d	552	10.5 d

the nominal power of 2 MW. The fourth, and main, cluster corresponds to the steady-state reactor noise established 1.7 days after the reactor begins operating at its full power and lasting up until the reactor cycle ends. For this fourth cluster, the noise intensity varies in time, tending to decrease by ~12% by the end of the cycle; this decrease in noise only slightly affects the spectral composition of the noise. Thus, the power noise is generally stabilized in 1.7 days. The characteristics of the four clusters are presented in Table 1. The cluster structures are shown in Fig. 7, "compressed" from the 256-dimensional to the two-dimensional space.

Fig. 8 shows the variation in cluster structure in the two-dimensional representation of the reactor noise space as a function of reactor operation time for both the total power fluctuations and the fluctuations that are due to vibrations of the movable reflectors.

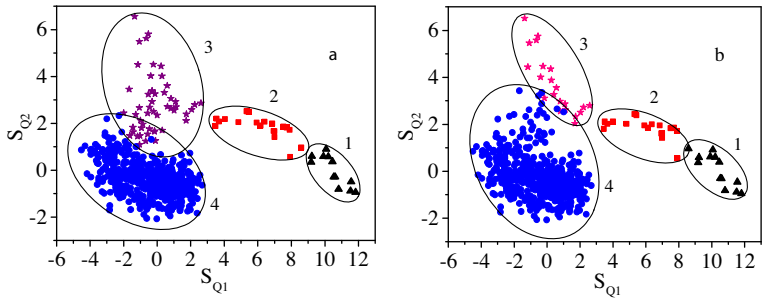

Fig. 7. Cluster structures compressed from the 256-dimensional to the two-dimensional space for the total pulse energy fluctuations (a) and the fluctuations due to axial vibrations of the MMR and AMR blades (b).

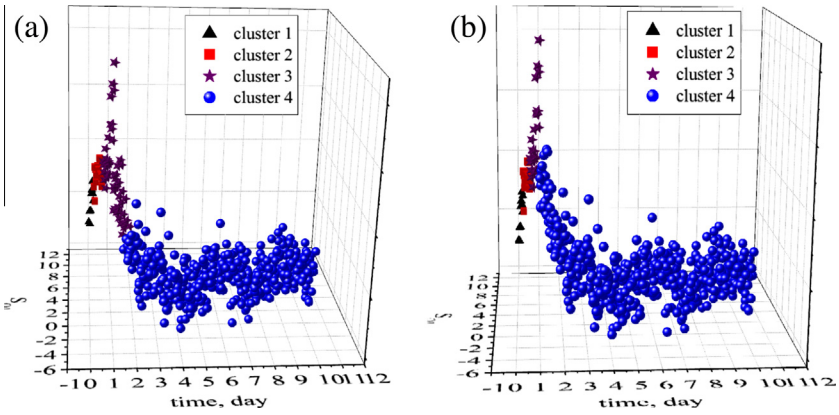

Fig. 8. Variation in the cluster structure of the pulse energy fluctuations as a function of time in the two-dimensional representation of the noise space for the total fluctuations (a) and the fluctuations due to vibrations of the MMR and AMR blades (b).

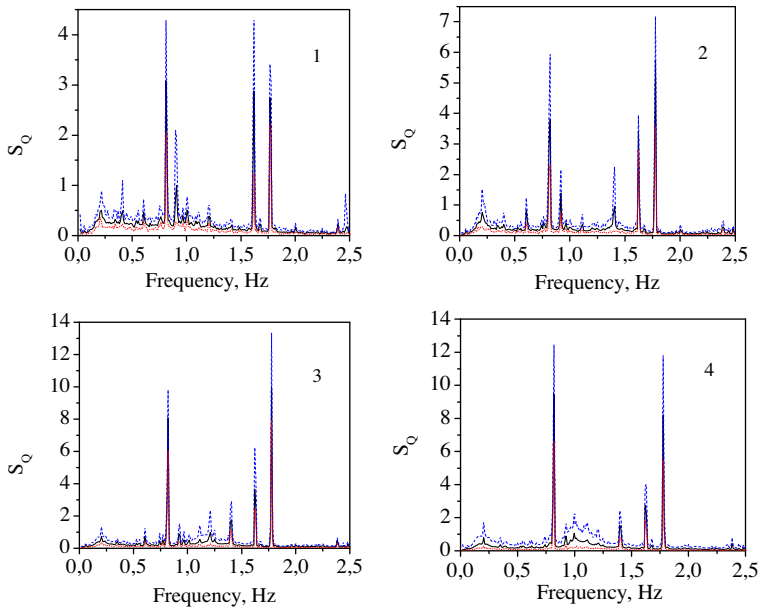

Fig. 9. Power spectral densities of the total pulse energy fluctuations corresponding to the centers of four clusters (cluster numbers are given in the figure). Dashed lines show the spread of the spectra in the clusters.

Fig. 9 shows centers of clusters with the minimum and maximum values of the spectra entering into the clusters. These figures show the spread of the spectra in the clusters. The following is evident from the Fig. 9 shown above. The centers of the first and second clusters are significantly different from those of the third and fourth clusters, with the centers of the third and fourth clusters being similar. The first two clusters, with the sharp variation in the center, correspond to the transition noise region ~0.5 day

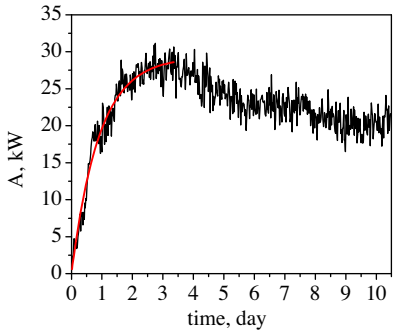

Fig. 10. Variation in the amplitude of pulse energy fluctuations (A, kW) at a frequency of 0.82 Hz as a function of the IBR-2M operation time after the nominal power of 2 MW is reached. Exponential approximation of the increase in the amplitude is given.

long after the reactor has reached maximum power. The third cluster, in the interval of 14–41 h (1.2 d) after the power has been reached, represents the reactor noise state that is close in structure to the fourth cluster. The total noise stabilization time is about 27 h (1.7 days). The cluster structure in the dominant spectrum coordinates, i.e., for the pulse energy fluctuations due to the vibrations of the movable reflectors, is similar to the structure of the total fluctuations (see Figs. 7 and 8). Therefore, the above analysis totally applies to this structure as well. Thus, the dynamic change in the noise state of the IBR-2M reactor, after reaching maximum power, is due to the vibration state of the movable reflectors.

As is evident from Figs. 4 and 6, it is the amplitude of the dominant fluctuations at the frequencies of 0.82 and 1.63 Hz that varies to a large extent. The variation in the amplitude of the fluctuations at these frequencies, as a function of reactor operation time, is shown in Fig. 10. In the first three days of reactor operation, the amplitude of the fluctuations, at a frequency of 0.82 Hz, asymptotically increases from ~0 to 30 kW with a constant of ~1 d; this pulse energy noise arises from vibrations of the movable reflectors (Pepelyshev, 1987). This noise feature is most likely to be due to thermomechanical deformations of the movable reflector drive, which is also supported by the following: for the previous mobile reflector version, where the AMR was a trident and the MMR was a blade, the dispersion and, thus, the amplitude of the axial AMR vibrations- asymptotically increased with the reactor operation time, as is also the case for the current version (MMR is a trident, and AMR is a fork) (Pepelyshev, 1988). Note that the observed frequencies in the power fluctuation spectrum are the masked analogues of some real frequencies folded into a frequency range below the critical Nyquist frequency, which – in our case – is 2.5 Hz.

The dominant frequency of 0.82 Hz can only be identified with a significant degree of uncertainty, since the characteristic real frequencies of the MMR and AMR vibrations are obviously higher than the critical frequency. According to (Pepelyshev, 1987), a probable analogue of the 0.82 Hz frequency can be the ~85 Hz frequency of one of the AMR eigenmodes, while the 1.63 Hz frequency can be associated with a small defect in the rotation gear box of the movable reflectors.

In order to perform a final comparison with the spectrum clustering results presented in Fig. 4, one more reactor operation cycle was investigated in 2013 (see Fig. 11). This cycle differs from the previous one in that it involves power dumping.

4. Conclusions

Cluster analysis of the IBR-2M pulse energy noise yielded data on the variation dynamics of the reactor noise state in a typical operation cycle. The noise state of the IBR-2M represented as the power spectrum of pulse energy fluctuations per cycle (~11 days) has a transition region that arises after the reactor reaches the nominal power of 2 MW. Transition region was characterized by a significant increase in the level of pulse energy fluctuations at the first day of reactor operation. The power noise is successively divided into three to four stable structures (clusters). The first two clusters are observed between 0 and 14 h after the maximum power has been reached. Then, 1.2 days later, the transition region ends, and the reactor noise state is stabilized 1.7 days after the maximum power is reached. The reactor operates in this state until the end of the cycle. It is shown that the transition region of the reactor noise is caused by a change in the vibration state of the movable reflectors, namely, by the axial vibrations of the reflector blades at frequencies of 0.82 and 1.40 Hz and in the range of 1.55–1.80 Hz. The main component in the transition region of the noise variation is the variation in the amplitude of the axial vibrations of the auxiliary movable reflector at frequencies of 0.82 and 1.63 Hz. For three days of reactor operation, the amplitude of the harmonic pulse energy fluctuations- at a frequency of 0.82 Hz- increases asymptotically from ~0 to ~30 kW with a constant of ~1 d. The aforementioned pulse energy frequencies constitute "hidden" frequencies, the analogues of which are higher frequencies of eigenmodes of the movable reflectors. The transition region of the reactor noise is most likely to be due to bending deformations of the movable reflectors occurring in the process of their heating after the maximum power is reached. It is also worth mentioning that the variation dynamics of the reactor noise state only slightly

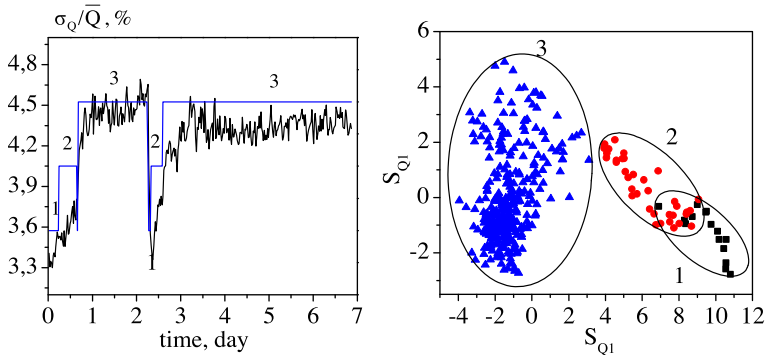

Fig. 11. Variation in the relative root-mean-square deviation of the total pulse energy fluctuations, and in the cluster exchange, as a function of the reactor operation time in the cycle with power dumping (left), and the clusters compressed from the 256-dimensional to the two-dimensional space of pulse energy noise (right). The numbers denote clusters.

vary from cycle to cycle and are only slightly affected by power dumping. The analysis shows that the variations are small and do not generally affect the safety of the reactor operation.

References

Anan'ev, V.D., et al., 2012. Physical startup of the upgraded IBR-2 reactor (IBR-2M). JINR Communication R13-2012-41, Dubna.

Anan'ev V.D., et al., 2012. Power startup of the upgraded IBR-2 reactor (IBR-2M). JINR Communication R13-2012-42, Dubna.

Boldak, A.A., Sukharev, D.L., 2011. Determination of the number of clusters in statistical data. Visnik KPI Ser. Informatika, upravlinnya ta obchislyuvalna tekhnika 53, 118–122.

Dunn, J., 1974. Well separated clusters and optimal fuzzy partitions. J. Cybern. 4, 95–104.

Gonzalez, R.C., Pry, D.N., Kryter, R.C., 1974. IEEE Trans. Nucl. Sci. NS-21(1), 1–8.

Goujun, Gan, Chaogun, Ma, Jianhong, Wu, 2007. Data Clustering: Theory, Algorithms, and Applications. vol. 2. pp. 94–137. vol. 4. pp. 354–362.

Lawrence Hubert, J., Hans-Friedrich, Köhn, Douglas Steinley, L., 2009. 20 Cluster Analysis: A Toolbox for MATLAB.

Pepelyshev, Yu.N., 1987. Investigation of vibrations of movable reflectors (energy startup of the IBR-2 reactor). JINR Communication 13-87-564, Dubna.

Pepelyshev, Yu.N., 1988. Time characteristics of the parameters of the power noise and vibrations of the movable reflectors of the IBR-2 reactor. JINR Communication R13-88-59, Dubna.

Pepelyshev, Yu.N., Dzwinel, W., 1990a. Pattern recognition application for surveillance of abnormal condition in a nuclear reactor. Ann. Nucl. Energy 18 (3), 117–123, 191.

Pepelyshev, Yu.N., Dzwinel, W., 1990. Clustering Method and Visualization Algorithms to Nuclear Reactor Operative Diagnostics. JINR Preprint E10-90-323, Dubna.

Pepelyshev, Yu.N., Dzwinelm, W., 1991. Pattern recognition system for the nuclear reactor noise image analysis and diagnostics. A Symposium on nuclear reactor surveillance and diagnostics, SMORNVT, May, 19–24. Gatlinburg, Tennessee, USA. Vol. 2 of 2.

Pepelyshev, Yu.N., Dzwinel, W., 1992. A pattern recognition approach to condition-based plant maintenance. Technical Committee Meeting on Safety and reliability Improvement through optimized Plant Maintenance. Vienna, Austria, 22–24 June.

Pepelyshev, Yu.N., Dzwinel, W., 1994. Pattern clustering and mapping for presentation of nuclear reactor noises. JINR Communication E10-94-61, Dubna.

Pepelyshev, Yu.N., Dzwinel, W., Jrsa, p., Rejchrt, J., 1994. Comparison of the noise diagnostic systems based on pattern recognition and discriminant methods. JINR Preprint E10-94-61, Dubna.

Rousseeuw, P.J., 1987. Silhouettes: a graphical aid to the interpretation and validation of cluster analysis. J. Comput. Appl. Math. 20, 53–65.

Wang, A., Wang, B., Peng, L., 2009. CVAP: validation for cluster analysis. Data Sci. J. 8, 88–93.